Romero-Gómez, P. [et al], "Semi-transparent polymer solar cells," Journal of Photonics for Energy 5(1), 057212 (16 February 2015). http://dx.doi.org/10.1117/1.JPE.5.057212

Copyright 2015 Society of Photo Optical Instrumentation Engineers (SPIE). One print or electronic copy may be made for personal use only. Systematic reproduction and distribution, duplication of any material in this publication for a fee or for commercial purposes, or modification of the contents of the publication are prohibited.

Romero-Gómez, P. [et al], "Semi-transparent polymer solar cells," Journal of Photonics for Energy 5(1), 057212 (16 February 2015). http://dx.doi.org/10.1117/1.JPE.5.057212

Semitransparent Polymer Solar Cells

Pablo Romero-Gómez[1], Francesco Pastorelli[1], Paola Mantilla-Pérez[1], Marina Mariano[1], Alberto Martínez-Otero[1], Xavier Elias[1], Rafael Betancur[1], and Jordi Martorell[1,2]

[1]*ICFO-Institut de Ciencies Fotoniques, Mediterranean Technology Park, 08860 Castelldefels (Barcelona), Spain.*
[2]*Departament de Fisica i Enginyeria Nuclear, Universitat Politècnica de Catalunya, Terrassa, Spain.*

Abstract. Over the last three decades progress in the organic photovoltaic field made apparent some device features which make organic cells applicable in electricity generation configurations where the standard Si based technology is not suitable. As for instance when a semitransparent photovoltaic panel is needed. When thin film solar cell performance is evaluated in terms of the device visible transparency and power conversion efficiency, the organic one offers the most promising solution. During the last three years research in the field has consolidated several approaches for the fabrication of high performance semitransparent organic solar cells. We have grouped them under three categories: devices where the absorber layer includes near infrared absorption polymers, devices incorporating 1-dimensional photonic crystals, and devices with a metal cavity light trapping configuration, which we review.

Keywords: photovoltaic cells; solar cells; transparent materials; organic materials; optical trapping; photonic crystals.

Address all correspondence to: Prof. Jordi Martorell, ICFO-Institut de Ciencies Fotoniques, Organic Nanostructured Photovoltaics, Av. Carl Friedrich Gauss, num. 3, Castelldefels, Spain, 08860;
Tel: +34 935534049; Fax: +34 935534000; E-mail: Jordi.Martorell@icfo.es

1. Introduction

Research in organic photovoltaics (OPVs) triggered when it was proposed as one of the low cost alternatives to the silicon based PV technology. For about three decades, progress in the field made apparent some specific features of the organic cells, which are very interesting when considering them in uses where the silicon technology is less applicable. During those years, material science research successfully pushed the band gap of PV polymers from the near UV or visible towards the near infrared region (NIR). Nowadays, one may find several PV polymers, known in the field as "low band gap polymers", where the band gap is centered close to where the sun

photon flux is maximum.[1-35] When combined with certain derivatives of the fullerene molecule, single junction cells with power conversion efficiencies approaching 10% can be fabricated.[36-40] Amazingly, in the majority of such high performance single junction devices, the absorber layer, consisting of a bulk hetero-junction (BHJ) of the above mentioned polymers and fullerene derivatives, is typically no more than 100 nm thick. Visible light is partially transmitted through such thin absorber layers, making it possible to clearly see objects which appear to the viewer unaltered in shape or color. The potential for integration of such technology on transparent vertical surfaces, which dominate the landscape of any major city, is tremendous. Devices fabricated from other thin film PV technologies can be made semitransparent, too. But, when the solar cell performance is evaluated in terms of the power conversion efficiency (PCE) and the level and quality of the luminosity, corresponding to the integral of the transmission weighted by the product of the human eye photopic spectral response with illumination from the white standard illuminant CIE-D65,[41] the organic technology offers the most promising solution.

Approximately ten years ago, attempts to fabricate semitransparent OPV cells could already be found in the scientific literature. Provided the intrinsic semi-transparency of the absorber layer, one of the main challenges researchers had to face was to obtain a good quality semitransparent top electrode. This electrode must be deposited when the absorber layer has already been deposited on the substrate and a non-aggressive deposition procedure needs to be used. Several different options have been considered such as low-temperature annealed ITO,[42-48] a three layer architecture combining a dielectric layer, an ultra thin metal layer and a second dielectric layer,[49-64] PEDOT,[65-67] silver grid,[68] Graphene,[69-71] carbon nanotubes,[67,72] and silver nanowires (AgNW).[73-78] However, the need for a non-destructive deposition technique for the top semitransparent electrode is, probably, not the major issue that semitransparent OPV cells must solve before becoming an industrially viable solution. Indeed, when the top electrode of an OPV cell is made semitransparent, the capacity of the solar device to trap the electromagnetic field in the absorber layer diminishes. Irrespective of the type of semitransparent top electrode used this occurs at all wavelengths leading to devices exhibiting PCEs which are about 60% the one corresponding to an equivalent opaque cell. During the last two or three years research in the field has consolidated several research approaches to partially limit such dramatic loss in PCE.

We have grouped them under three categories. First we will consider what is, perhaps, the most straightforward approach consisting on further decreasing the polymer band gap to obtain a larger transparency in the visible.[79-81] One of the most relevant features of this approach is that it provides a very nice colorless high level of transparency. On the other hand, the limited harvesting at all wavelengths resulting from the low reflectivity top electrode can be partially compensated with the incorporation of an additional absorber layer in a tandem configuration.[82-85] The second approach to increase transparency in the visible and limit the loss in PCE is the incorporation of multilayer anti-reflection coatings for the visible or Bragg reflectors to help trap the near UV and NIR.[41,42,86-90] The combination of both may further improve the balance between transparency and PCE. But, an optimal performance is achieved when the multilayer structure is a non-periodic structure designed ad hoc.[41] In that latter case, an inverse integration design must be used to determine each layer thickness to be specific for the extinction coefficient of the absorber layers, the rest of materials used in the electrodes and buffer layers, and the architecture of the device as a whole. The last category we will discuss consists in enclosing the active layer in a Fabry-Perot type cavity formed by the two metallic semitransparent electrodes. This approach which, until recently, had been applied to opaque cells with limited success, in 2014 was proven to lead to high PCEs for opaque cells using low band gap polymers in the absorber layer.[91] The same approach has been applied to semitransparent devices and cells exhibiting a PCE equivalent to 90% the PCE of the opaque counterpart have been demonstrated.[92]

2. Semitransparent polymer cells

2.1 Semitransparent OPV cells with NIR absorption polymers

A straightforward strategy to fabricate semitransparent OPVs is to use donor polymers harvesting most of the photons in the NIR. In ref. 79 the authors used as absorber film a blend of PBDTT-DPP and PCBM. PBDTT-DPP is a low band gap polymer with strong photosensitivity in the 650-850 nm wavelength range, while the absorption of PCBM is located below 400 nm. With these two materials in combination, the PBDTT-DPP: PCBM photoactive layer has an average transmission

of 68% over the visible range (400 to 650 nm), but is strongly absorbing in the NIR range (from 650 to 850 nm). This spectral coverage of PBDTT-DPP:PCBM film ensures harvesting of UV and NIR photons leading to PCEs above 4%. More recently, the PCPDTFBT polymer with a similar spectral response, i.e. a major absorption located at the near infrared region, was used to fabricate semitransparent OPV cells with a PCE above 5%.[93] In the fabricated devices, PCPDTFBT:$PC_{71}BM$ was used as active BHJ layer, with a configuration of ITO/ZnO/PCPDTFBT:$PC_{71}BM$/PEDOT:PSS/ultra-thin Ag. With a 15 nm Ag as the semitransparent top electrode, the device exhibited an average transmission of 39.4% while for device with thinner Ag layer of 10 nm the average transmission was increased to 47.3% without compromising its PCE significantly. This finding was associated with the good wettability of Ag atoms on the polar PEDOT:PSS layer, which allowed Ag atoms to grow homogeneously.

Although the results reported above indicate the soundness of the NIR absorption polymer approach, to obtain high performance semitransparent cells, there is, however, a limit linked the decrease in harvesting capacity when a device incorporates two semi-transparent electrodes. This is the case because the semi-transparency of the electrodes is usually homogenously distributed in the UV-Visible-NIR range and the device loses its capacity to trap invisible UV or NIR light as well. To compensate for this effect, the authors of ref. 84 considered a transparent OPV having a tandem structure using two different polymers with an absorption band in the NIR. The front subcell in the device incorporated the transparent absorber PBDTT-FDPP-C12:PC61BM which exhibits an average visible transmission from 400 to 650 nm of approximately 60% and an IR transmission of 52% from 650 to 800 nm. Therefore, approximately half of the IR energy was not fully captured for energy conversion. The back subcell featuring PBDTT-SeDPP:PC61BM as the absorber exhibited a similar NIR transmission of 53% with extended NIR response from 650 to 900 nm. By stacking these two transparent absorbers in a tandem structure, NIR transmission dropped to 26%. In other words, the photon absorption efficiency in the NIR range increased nearly twofold and semitransparent OPV cells exhibiting a PCE above 7% were reported. Recently an efficiency of 8.02 % in a tandem OPV cell with a semi-transparency of 44.90% was achieved using solution-processed graphene as front electrode and laminated nanowires as top electrode.[71] In all such tandem

devices, the NIR energy was harnessed more completely, while transmitting approximately half of the visible photons.

2.2 Semitransparent OPV cells incorporating 1-D photonic crystals or multilayers

A manipulation of the photon propagation inside the cell can be achieved externally with the use of 1-D photonic crystals or dielectric multilayers. To enhance trapping of the electromagnetic field at the near UV and NIR wavelengths, one may consider 1-D photonic structures incorporated above the top semitransparent electrode to reflect the NIR and UV and transmit the visible. A combination of a Bragg reflector and an anti-reflective coating (ARC) has been used to increase NIR photon harvesting demonstrating that the efficiency of small molecule OPV cells could be increased from 1.3% to 1.7%.[42] Similar configurations considered the use of a single Bragg mirror deposited on top of the back metal electrode to reflect the red and NIR wavelengths. This was shown to increase the short circuit current density (J_{sc}) of OPVs as the number of layers was increased from 2 to 8.[86]

The 1-D photonic crystals or Bragg reflectors are designed to satisfy the Bragg condition to get maximum reflectivity at a NIR wavelength. However, in a photovoltaic device interference must be the optimal one at all wavelengths of interest to achieve the highest visible transmission and an optimal trapping for UV and IR light. One way to better reach the goal of a broadband photonic control using simple one-dimensional structures is to increase the degrees of freedom and use a numerical inverse problem solving method. For a semitransparent OPV cell there are essentially two parameters that will determine its level of performance: the efficiency in converting light to electricity and the device visible transmission or luminosity. The numerical inverse problem solving must be implemented by removing the periodicity constraint to design a photonic multi-layer (cf. Figure 1) that maximizes the contribution to the J_{sc} for wavelengths below near UV and above NIR while keeping the device visible transparency above the desired lower limit value.

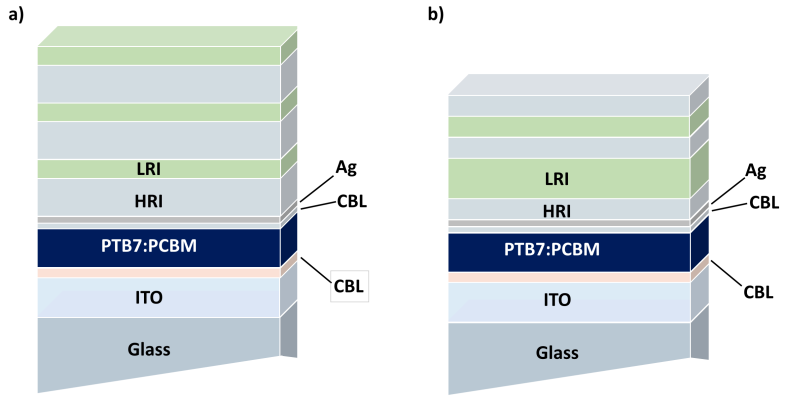

Figure 1 PTB7:$PC_{71}BM$ cells incorporating **a**) a periodic 1-D photonic crystal of six layers, and **b)** a non-periodic multilayer of five layers. LRI and HRI indicate low and high refractive index, respectively. CBL indicates charge blocking layer. When the bottom CBL is an electron blocking layer the configuration is known to be a standard one, while when the top CBL is an electron blocking layer the configuration is known as inverted.

In an application to semitransparent OPV cells of the inverse solving method, single junction cells using absorber layers of the PTB7:$PC_{71}BM$ blend were considered.[41] As shown in Figure 2, the J_{sc} obtained following such procedure increases rapidly when layers are added in the photonic crystal but, saturates beyond five layers. For the five layer structure, the calculated J_{sc} was 76.3% that of the corresponding opaque cell. On the contrary, for an optimal six layer periodic structure, the best efficiency that can be reached is 72% that of the opaque cell. The better performance of the non-periodic structure is attributed to a reflectivity, shown in Figure 3, that adapts optimally, not only to the absorption spectrum of the absorber blend but also to the sun photon flux. As seen in Figure 3 the reflectivity of the non-periodic structure is enhanced for the NIR photons at the expense of a reduction for the near UV photons when compared to the reflectivity of the six layer periodic structure. This result is in correspondence to a larger photon flux in the NIR range relative to the UV. The reflectivity in the visible is maintained low in both cases, ensuring a visible device transparency or luminosity close to or above 30%.

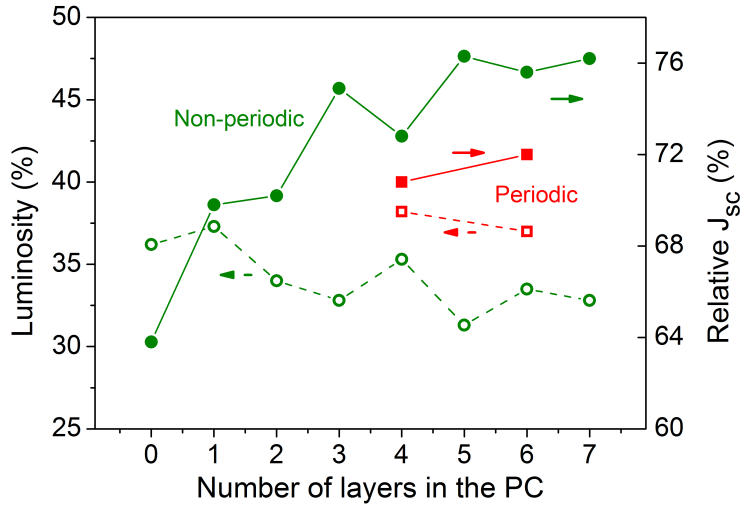

Figure 2 As a function of the number of layers numerically determined relative short circuit current (green solid dots) and luminosity (green circles) for devices incorporating the non-periodic multilayer, and relative short circuit current (red solid squares) and luminosity (red empty squares) for devices incorporating optimal periodic 1-D photonic crystals of 2 and 3 periods. The short circuit currents are given relative to the corresponding one from an equivalent opaque cell.

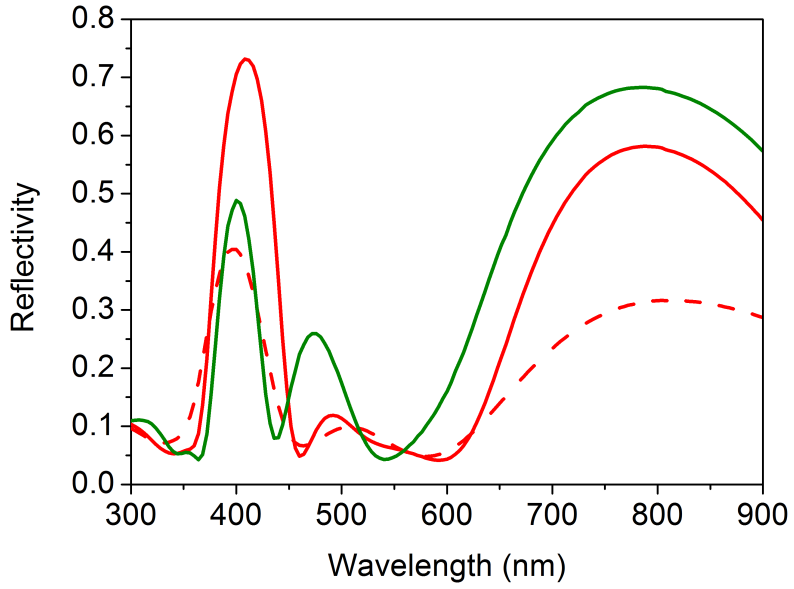

Figure 3 Reflectivity of the periodic 1-D photonic crystal of four layers (red dashed line), of six layers (red solid line) and a non-periodic multilayer of five layers (green solid line). All three structures where designed to maximize

the performance of the entire OPV device using the same inverse integration. The constraint of periodicity was removed for the last case.

This type of design has been tested and implemented in cells constructed either in a standard or inverted configuration using the PTB7:$PC_{71}BM$ blend as the absorber layer. For the standard configuration ITO and a 10 nm thick Ag layer were used as electrodes while PEDOT:PSS and thermally evaporated BCP were used as electron blocking layer (EBL) and hole blocking layer (HBL), respectively. The multilayer structure implemented on top of the Ag electrode combined layers of a low refractive index material as LiF with layers of high refractive index material as MoO_3. As shown in Figure 4a, where the calculated external quantum efficiency (EQE) of the cell including the multilayer is compared to the EQE of a semitransparent cell not including the multilayer, one observes that contributions to J_{sc} from the NIR as well as near UV photons are clearly enhanced. For certain NIR photons the EQE for the device incorporating the multilayer is close to match the EQE of an equivalent opaque cell.[41] On the other hand, contribution from visible photons to the EQE remains similar to the one seen for bare semitransparent cell for the same type of photons.

a) **b)**

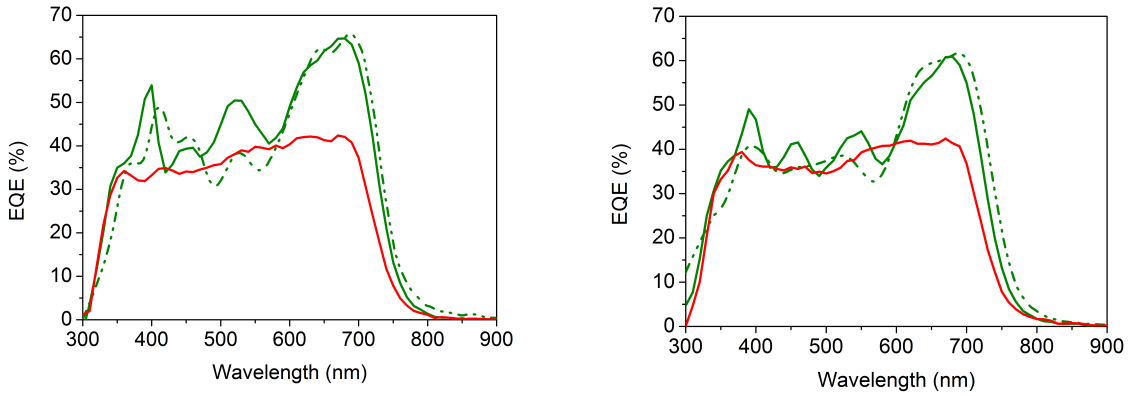

Figure 4 a) Experimentally measured EQE for semi-transparent cells in the standard configuration when no photonic management is incorporated (red solid line), and when a 1-D non-periodic crystal of five layers is included (green solid line). Numerically predicted EQE for a semi-transparent standard cell incorporating a 1-D non-periodic crystal of five layers designed ad hoc to optimize visible transparency and PCE (green dashed line). **b**) Same as in a) but for an inverted configuration.

For the inverted solar cells, the architecture considered was similar except that a thermally evaporated MoO_3 layer was used as EBL while a ZnO layer was used as HBL. The ZnO layer was grown by sol-gel where the precursor solution was prepared according to Ref. 94. In order to make the inverted devices semitransparent, similarly to the standard configuration the back silver contact was made 10 times thinner than for the opaque cells, i.e. 10 nm instead of 100 nm thickness. To enhance the performance of the semitransparent cells a five-layer structure based on MoO_3 (high refractive index material) and MgF_2 (low refractive index material) was incorporated. The EQE shown in Figure 4b shows a similar redistribution of photon harvesting as the one found for the standard configuration devices. In both cases, as seen in Figure 4, the agreement between the experimentally measured EQE and the numerical design is remarkable.

2.3 Semitransparent OPV cells with light trapping metal cavities

Light trapping by using two metal electrodes has been considered in several OPV opaque cell configurations. Recently, OPV devices with an ITO-free microcavity structure that reached high PCEs of 8.5% on, both, glass and flexible plastic substrates have been reported.[91] This corresponds to ~20% improvement in PCE when compared to the equivalent ITO-based devices. The significantly enhanced performance was ascribed to the substantially improved photon collection by the resonant microcavity structure, which contributed to improved photocurrent compared with devices built on ITO-coated substrates.

Photon trapping in between two metal electrodes can also be applied to semi-transparent OPV cells. In that event both electrodes in the device are kept sufficiently thin to ensure a sufficiently high luminosity. In a recent implementation of this configuration, to increase light trapping, an ARC was deposited on top of the front metal contact while a non-periodic multilayer was inserted in between the back metal contact and the substrate. As for the configuration considered in the previous section, the optimal layer distribution was designed specifically for the cell architecture used. With a device architecture as the one shown schematically in Figure 5, semi-transparent cells whose PCE was 5.3%, corresponding to 90% the PCE of the corresponding opaque cell were reported.[92] The visible transparency of such cells

differed little from the semi-transparent cell which did not include the multilayer, while the EQE closely matched that of the opaque cell as seen in Figure 6. The opaque cell was in an inverted configuration with the following architecture: As active material a thin layer of PTB7:$PC_{71}BM$ blend was used. The bottom electrode was an opaque layer of 120 nm of Au and the top electrode was a semi-transparent layer of 10 nm of Ag. ZnO and MoO_3 were used as HBL and EBL, respectively. On top of the Ag electrode a two-layer ARC made of MoO_3 and LiF was deposited. For the semi-transparent devices the exact same architecture was used except that the Au electrode was thinned down to 13 nm. As seen in Figure 5, in between the Au electrode and the substrate a six-layer 1-D multilayer made alternating TiO_2 and SiO_2 was incorporated. Following an inverse integration procedure as discussed above such structure was designed numerically to maximize the current while keeping the luminosity of the solar cell above 20%.

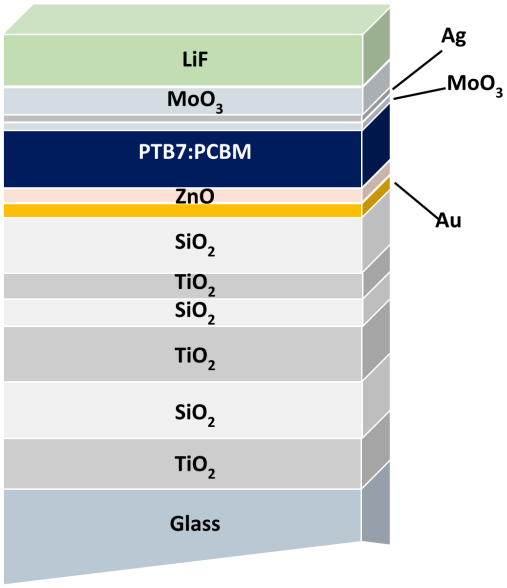

Figure 5 Schematic picture of a PTB7:$PC_{71}BM$ cell in a metal cavity configuration incorporating a periodic 1-D photonic crystal of six layers and an anti-reflection coating.

The conclusion was that when the OPV architecture included two thin metallic electrodes, one of them being assisted with 1-D multilayer to enhance reflectivity for the case of semi-transparent cells, one may obtain a broadband photon trapping capacity sufficient to match the performance of semi-transparent cells to opaque ones.

It was demonstrated that it is the combined effect of such 1-D multilayer and a thin metal layer that prevents, to a large extent, the loss in photon harvesting capacity exhibited by the majority of semi-transparent cells. Indeed, the J_{sc} for a cell device incorporating such cavity configuration, which exhibited a 21% luminosity amounted to 96.4% the J_{sc} of the corresponding opaque cell.

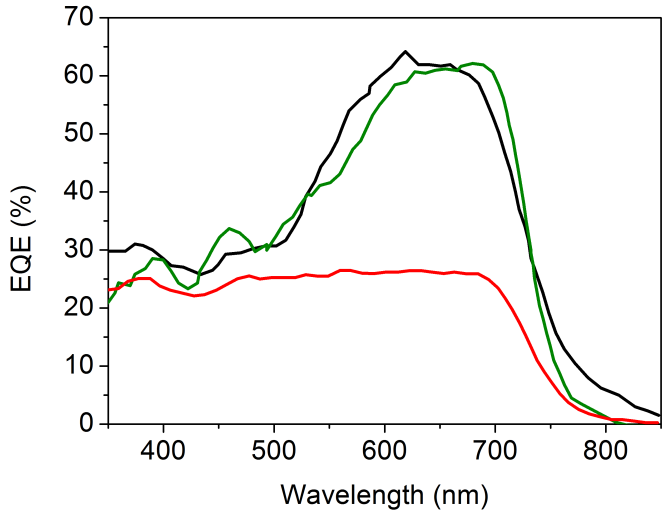

Figure 6 Experimentally measured EQEs of an opaque cell (black solid line), of a bare semi-transparent cell (red solid line) and a semi-transparent cell in a metal cavity configuration (green solid line), as the one shown in Figure 5, incorporating a periodic 1-D photonic crystal of six layers and an anti-reflection coating.

3. Towards fully solution processed semi-transparent OPV cells

A summary of the recent achievements in OPV is given in Table 1. From that table we may conclude OPV cells with transparencies above 30% combined with PCE above 5% are feasible by the implementation of different kind of approaches. It would make sense to combine the approach based on using NIR absorber layers with the one based on incorporating a photonic structuration to re-harvest the near UV and NIR light lost when the top electrode is made semi-transparent; this approach would push the PCE of highly semi-transparent cells closer to the corresponding PCE for the

opaque devices, bringing the PCE of visibly transparent cells to the limit efficiencies that were recently established on a model based on the Schockley-Queisser theory.[95] However, there are, several scientific and technical issues that must be addressed before such OPV technology can become commercially applicable in any kind of semi-transparent device or element. Although the PCEs measured are considerably high (See Table 1), a drop of at least 20% in PCE is likely to happen when up-scaling from laboratory cells to modules. In the majority of the configurations from Table 1, the fabrication procedure followed includes several steps that require high vacuum thermal evaporation or sputtering, especially in the fabrication of the electrodes. It is likely that this would preclude a favorable cost efficiency ratio when this technology is compared to other thin-film inorganic based technologies that also have the potential to become semitransparent.

Several relevant steps in that direction have been achieved recently when a solution processing was implemented in all the fabrication steps for highly transparent cells. AgNW were used as the material in the semi-transparent electrodes on both sides of the OPV cell.[77,96] and, more recently, other alternatives to high vacuum processed transparent electrodes such as conducting polymer electrode,[73] silver grids,[68] or graphene,[69-71] have been implemented in OPV cells. In general, the fully solution-processed cells have been shown to perform similarly to equivalent cells fabricated using a sputtered ITO electrode.

On the other hand, although some companies or research centers are working towards improving the stability of the OPV cells, there are no systematic studies that demonstrate an optimal performance of OPV devices over the long timescales required for the majority of applications of transparent PV cells. Finally, it will be necessary to address other relevant issues related to the product life cycle, such as safe disposal and recovery of the materials used in the fabrication of OPVs. In summary, to achieve an industrial production of a semi-transparent PV technology the main challenges are to increase the efficiency, ,establish and implement the appropriate up-scaling methodology and obtain devices stable whilst ensuring a low cost production.

Table 1 Summary of high performance semitransparent OPV cells reported during the 2012-2014 period

Structure	J_{sc} *(mA/cm^2)*	V_{oc} *(V)*	*FF*	*Eff (%)*	*Transmission (%)*	*Ref.*
ITO/PEDOT:PSS/PBDTT-DPP:PCBM/TiO2/AgNW	9.30	0.77	56.2	4.0	60 (at 550 nm)	79
ITO/PEDOT:PPS/ PIDT-PhanQ:$PC_{71}BM$/Surfactant/thin Ag	9.99	0.84	61	5.1	24 Avg. visible	81
ITO/ZnO/PCPDTFBT:$PC_{71}BM$/ PEDOT:PPS/thin Ag	11.9	0.73	58.3	5.1	39.4 Avg. 380-700 nm	93
ITO/PEDOT:PSS/ PBDTT-FDPP-C12:PC61BM /PFN/TiO2/PEDOT/ PBDTT-SeDPP:PC71BM/TiO_2/AgNW	8.4	1.47	59	7.3	30 Avg. 400-650 nm	84
Graphene Mesh/PEDOT:PSS/ PSEHTT/IC60BA/ZnO/PEDOT:PSS/ PBDTT-DPP:PC71BM/TiO2/AgNW	7.62	1.62	64.2	8.02	45 Avg. 400-650 nm	71
ITO/ZnO/P3HT:PCBM/MoO_3/thin Ag/1-D photonic crystal	10.89	0.63	66	4.3	12 At 550 nm	90
ITO/PEDOT/PTB7:$PC_{71}BM$/BCP/thin Ag/1-D photonic crystal	10.9	0.733	70	5.6	28 Luminosity	41
1-D photonic crystal /thin Au/ZnO/ PTB7:$PC_{71}BM$/MoO_3/thin Ag/ARC	10.7	0.728	67.9	5.3	21.4 Luminosity	92

The goal in the following years is to combine, in a fully solution processed single device, NIR polymers with photonic structures or 1-D multilayers. This will require the development of new nano-materials that can be solution processed to fabricate the buffer layers (HBL and EBL) and the photonic multi-layered architecture. The aim should be to completely eliminate all of the high vacuum steps. Indeed, fabrication using only solution processing may be critical when considering transparent devices with possible applications as building elements, provided the production of large window panels using high vacuum technology is costly and technically complex. The challenge of enhancing the performance of semi-transparent cells also requires an improvement of the performance of opaque cells. To achieve such a goal one may target the development of new cross-linkable absorber polymers adapted to better light harvesting in the NIR. To complement this approach, one may develop optically optimized tandem architectures to increase light harvesting.

Acknowledgements

The authors acknowledge support from the Ministerio de Economia y Competitividad (grants MAT2011-28665, IPT-120000-2010-29, IPT-2012-0986-120000 and CSD2007-00046).

References

1. N. Blouin et al., "Toward a rational design of poly(2,7-carbazole) derivatives for solar cells" J. Am. Chem. Soc. **130** (2) 732-742(2008).
2. K. H. Hendriks et al., "Small-Bandgap Semiconducting Polymers with High Near-Infrared Photoresponse" J. Am. Chem. Soc., **136**, 12130−12136 (2014).
3. K. H. Hendriks et al., "High-Molecular-Weight Regular Alternating Diketopyrrolopyrrolebased Terpolymers for Efficient Organic Solar Cells" Angew. Chem. Int. Ed., **52**, 8341–8344 (2013).
4. S.H. Park et al., "Bulk heterojunction solar cells with internal quantum efficiency approaching 100%" Nat. Photonics **3** 297 - 302 (2009).
5. Q. Ruiping et al., "A Planar Copolymer for High Efficiency Polymer Solar Cells" *J. Am. Chem. Soc.* **131** (41) 14612–14613(2009).
6. H.J. Son et al., "Synthesis of fluorinated polythienothiophene- co - benzodithiophenes and effect of fluorination on the photovoltaic properties" J. Am. Chem. Soc. **133** (6) 1885-1894 (2011).
7. Weiwei Li et al., "Universal Correlation between Fibril Width and Quantum Efficiency in Diketopyrrolopyrrole-Based Polymer Solar Cells" J. Am. Chem. Soc. 135, 18942−18948, (2013).
8. S. Albrecht et al., "Fluorinated copolymer PCPDTBT with enhanced open-circuit voltage and reduced recombination for highly efficient polymer solar cells" J. Am. Chem. Soc. 134 (36) 14932-14944 (2012).
9. P.M Beaujuge et al., "Tailoring structure-property relationships in dithienosilole- benzothiadiazole donor-acceptor copolymers" J. Am. Chem. Soc. 131 (22) 7514-7515 (2009).
10. L. Ying et al., "Regioregular pyridal[2,1,3]thiadiazole π-conjugated copolymers" J. Am. Chem. Soc. 133 (46) 18538-18541 (2011).

11. Weiwei Li et al., “Enhancing the Photocurrent in Diketopyrrolopyrrole-Based Polymer Solar Cells via Energy Level Control” J. Am. Chem. Soc. 134, 13787−13795 (2012).
12. M. Wang et al., “Donor-acceptor conjugated polymer based on naphtho[1,2-c:5,6- c]bis[1,2,5]thiadiazole for high-performance polymer solar cells” J. Am. Chem. Soc. 133 (25) 9638-964 (2011).
13. Osaka et al., “Synthesis, characterization, and transistor and solar cell applications of a naphthobisthiadiazole-based semiconducting polymer” J. Am. Chem. Soc. **134** (7) 3498-3507(2012).
14. B. Carsten et al., “Mediating solar cell performance by controlling the internal dipole change in organic photovoltaic polymers” Macromolecules **45** (16) 6390-6395 (2012).
15. L.M. Campos, et al., “Extended Photocurrent Spectrum of a Low Band Gap Polymer in a Bulk Heterojunction Solar Cell” Chem. Mater. 17 4031–4033 (2005).
16. H. Zhong, Z. et al., “Fused Dithienogermolodithiophene Low Band Gap Polymers for High-Performance Organic Solar Cells without Processing Additives” J. Am. Chem. Soc. 135 2040–2043 (2013).
17. K. H. Hendriks et al., “Homocoupling Defects in Diketopyrrolopyrrole-Based Copolymers and Their Effect on Photovoltaic Performance” J. Am. Chem. Soc. 136, 11128−11133 (2014).
18. J. Hou et al., “Synthesis, characterization, and photovoltaic properties of a low band gap polymer based on silole-containing polythiophenes and 2,1,3-benzothiadiazole” J. Am. Chem. Soc. **130** (48) 16144-16145 (2008).
19. R.C. Coffin et al., “Streamlined microwave-assisted preparation of narrow-bandgap conjugated polymers for high-performance bulk heterojunction solar cells” Nat. Chemistry 1(8), 657-661 (2009).
20. L. Huo et al., “Low band gap dithieno[3,2-b:2′,3′-d]silole-containing polymers, synthesis, characterization and photovoltaic application” Chem. Commun. **37**, 5570-5572 (2009).
21. G.C Welch et al., “Lewis acid adducts of narrow band gap conjugated polymers” J. Am. Chem. Soc. **133**, 12, 4632-4644 (2011).
22. Z.B. Henson et al. “Pyridalthiadiazole-based narrow band gap chromophores” J. Am. Chem. Soc. **134** (8) 3766-3779 (2012).

23. H. Brisset et al., Novel narrow bandgap polymers from sp3 carbon-bridged bithienyls: Poly(4,4-ethylenedioxy-4H-cyclopenta[2,1-b;3,4-b′]dithiophene) J. Am. Chem. Soc. **11**, 1305-1306(1994).
24. S. Esiner et al., "Quantification and Validation of the Efficiency Enhancement Reached by Application of a Retroreflective Light Trapping Texture on a Polymer Solar Cell" Adv. Energy Mater. 3, 1013–1017 (2013)
25. Y. Liang et. al., "Highly efficient solar cell polymers developed via fine-tuning of structural and electronic properties" J. Am. Chem. Soc. **131** (22) 7792-7799 (2009).
26. H.-Y Chen et al., "Polymer solar cells with enhanced open-circuit voltage and efficiency" Nat. Photonics **3** (11) 649-653 (2009).
27. Y. Liang et al., "For the bright future-bulk heterojunction polymer solar cells with power conversion efficiency of 7.4%" Adv. Mater. **22** (20) E135-E138 (2010).
28. B. Carsten et al., "Examining the effect of the dipole moment on charge separation in donor-acceptor polymers for organic photovoltaic applications" J. Am. Chem. Soc. **133** (50) 20468-20475 (2011).
29. H. Zhou, et al., "Development of fluorinated benzothiadiazole as a structural unit for a polymer solar cell of 7% efficiency" Angew. Chem. **50** (13) 2995-2998 (2011).
30. S.C. Price et al., "Fluorine substituted conjugated polymer of medium band gap yields 7% efficiency in polymer-fullerene solar cells" J. Am. Chem. Soc. **133** (12) 4625-463 (2011).
31. A.C. Stuart et al., "Fluorine substituents reduce charge recombination and drive structure and morphology development in polymer solar cells" J. Am. Chem. Soc. **135** (5) 1806-1815 (2013).
32. L. Huo et al., "A Poh benzo[1,2-6:4,5-b′]dithiophene derivative with deep HOMO level and its application in high-performance polymer solar cells" Angew. Chem. **49** (8) 1500-150(2010).
33. L. Huo et al., "Replacing alkoxy groups with alkylthienyl groups: A feasible approach to improve the properties of photovoltaic polymers" Angew. Chem. **50** (41), 9697-9702 (2011).
34. L. Dou et al., "Systematic investigation of benzodithiophene- and diketopyrrolopyrrole- based low-bandgap polymers designed for single

junction and tandem polymer solar cells" J. Am. Chem. Soc. **134** (24) 10071-10079 (2012).

35. L. Yongye et al., "For the Bright Future—Bulk Heterojunction Polymer Solar Cells with Power Conversion Efficiency of 7.4%" Adv. Mater., **22**, E135–E138 (2010).
36. L. Shengjian et al., "High-Efficiency Polymer Solar Cells via the Incorporation of an Amino-Functionalized Conjugated Metallopolymer as a Cathode Interlayer" J. Am. Chem. Soc. **135** 15326−15329 (2013).
37. C. Hyosung et al., "Multipositional Silica-Coated Silver Nanoparticles for High-Performance Polymer Solar Cells" Nano Lett. **13**, 2204−2208 (2013).
38. H. Zhicai et al., "Enhanced power-conversion efficiency in polymer solar cells using an inverted device structure" Nat. Photonics **6**, 591-595 (2012).
39. H. Zhicai et al., "Simultaneous Enhancement of Open-Circuit Voltage, Short-Circuit Current Density, and Fill Factor in Polymer Solar Cells" Adv. Mater. **23**, 4636–4643 (2011).
40. L. Lu and L. Yu, "Understanding Low Bandgap Polymer PTB7 and Optimizing Polymer Solar Cells Based on It" Adv. Mater. **26** (26) 4413 (2014).
41. R. Betancur et al., "Transparent polymer solar cells employing a layered light-trapping architecture" Nature Photonics **7**, 995–1000 (2013).
42. R. R. Lunt & V. Bulovic "Transparent, near-infrared organic photovoltaic solar cells for window and energy-scavenging applications" Appl. Phys. Lett. **98**, 113305 (2011).
43. J. Huang et al., "A Semi-transparent Plastic Solar Cell Fabricated by a Lamination Process" Adv. Mater. 20, 415–419 (2008).
44. Bailey-Salzman et al., "Semitransparent organic photovoltaic cells" Appl. Phys. Lett., **88** (23), 233502–3 (2006).
45. G.-M. Ng et al., "Optical enhancement in semitransparent polymer photovoltaic cells" Appl. Phys. Lett. **90** (10), 103505–3 (2007).
46. G. Gu et al., "Transparent organic light emitting devices" Appl. Phys. Lett. **68** (19), 2606–8 (1996).
47. F-C. Chen et al., "Polymer photovoltaic devices with highly transparent cathodes" Org.Electron. **9** 1132–1135(2008).

48. H. Schmidt et al., “Efficient semitransparent inverted organic solar cells with indium tin oxide top electrode” Appl. Phys. Lett. **94**, 243302 (2009).
49. C. Tao et al., “Semitransparent inverted polymer solar cells with MoO3/Ag/MoO3 as transparent electrode” Appl. Phys. Lett. **95**, 053303 (2009).
50. R. Koeppe et al., “Organic solar cells with semitransparent metal back contacts for power window applications” ChemSusChem. **2**(4) 309-13 (2009).
51. G. Li et al., “Efficient inverted polymer solar cells” Appl. Phys. Lett. 88 253503 (2006).
52. A. Colsmann et al., “Efficient semi-transparent organic solar cells with good transparency color perception and rendering properties” Adv. Energy Mater. **1**, 599–603 (2011).
53. N. P. Sergeant et al., “Design of transparent anodes for resonant cavity enhanced light harvesting in organic solar cells” Adv. Mater. **24**, 728–732 (2012).
54. K-S. Chen et al., “Strong Photocurrent Enhancements in Highly Effi cient Flexible Organic Solar Cells by Adopting a Microcavity Configuration” Adv. Mater. **26**, 3349–3354 (2014).
55. L. Shen, et al. Semitransparent polymer solar cells using V2O5/Ag/V2O5 as transparent anodes. Org. Electron. **12**, 1223–1226 (2011).
56. C. Tao et al. “Tailoring spatial distribution of the optical field intensity in semitransparent inverted organic solar cells” J. Phys. Chem. C **115**, 12611–12615 (2011).
57. S. Tanaka, et al. Semitransparent organic photovoltaic cell with carbon nanotube–sheet anodes and Ga-doped ZnO cathodes. Synth. Metals **159**, 2326–2328 (2009).
58. T. Winkler et al., “Efficient large area semitransparent organic solar cells based on highly transparent and conductive ZTO/Ag/ZTO multilayer top electrodes” Org. Electron. **12**, 1612–1618 (2011).
59. H. Jin et al., “Efficient large area ITO-and-PEDOT-free organic solar cell submodules” Adv. Mater. **24**, 2572–2577 (2012).
60. Z. Liu, et al., “The application of highly doped single-layer graphene as the top electrodes of semitransparent organic solar cells” ACS Nano **6**, 810–818 (2012).

61. B. O'Connor et al., "Transparent and conductive electrodes based on unpatterned, thin metal films" Appl. Phys. Lett., **93** (22), 223304–3 (2008).
62. J. Meiss et al., "Towards efficient tin-doped indium oxide (ITO)-free inverted organic solar cells using metal cathodes" Appl. Phys. Lett., **94** (1), 013303-3 (2009).
63. J. Meiss et al., "Optimizing the morphology of metal multilayer films for indium tin oxide (ITO)-free inverted organic solar cells" Appl. Phys. **105** (6), 063108-5 (2009).
64. A. Bauer et al., "ZnO: Al cathode for highly efficient, semitransparent 4% organic solar cells utilizing TiOx and aluminium interlayers" Appl. Phys. Lett. **100**, 073307 (2012).
65. Y. Zhou, et al., "Indium tin oxide-free and metal-free semitransparent organic solar cells" Appl. Phys. Lett. 97, 153304 (2010).
66. R. J. Peh et al., "Vacuum-free processed transparent inverted organic solar cells with spray-coated PEDOT: PSS anode" Sol. Energy Mater. Sol. Cells **95**, 3579–3584 (2011).
67. X. Hu et. al. "Large-Scale Flexible and Highly Conductive Carbon Transparent Electrodes via Roll-to-Roll Process and Its High Performance Lab-Scale Indium Tin Oxide-Free Polymer Solar Cells" Chem. Mater **26**, 6293-6302 (2014).
68. T. Ameri et al., "Fabrication, Optical Modeling, and Color Characterization of Semitransparent Bulk-Heterojunction Organic Solar Cells in an Inverted Structure" Adv. Funct. Mater. 20 1592–1598 (2010).
69. P. Lin et al., "Semitransparent organic solar cells with hybrid monolayer graphene/metal grid as top electrodes" Appl. Phys. Lett. **102**, 113303 (2013).
70. Y.-Y. Lee et al., "Top laminated graphene electrode in a semitransparent polymer solar cell by simultaneous thermal annealing/releasing method" ACS Nano **5**, 6564–6570 (2011).
71. A. R. b. M. Yusoff et. al."High-Performance Semitransparent Tandem Solar Cell of 8.02% Conversion Efficiency with Solution-Processed Graphene Mesh and Laminated Ag Nanowire Top Electrodes" Adv. Energy Mater. **4**, 16146840 (2014).

72. S. Tanaka et al., “Semitransparent organic photovoltaic cell with carbon nanotube-sheet anodes and Ga-doped ZnO cathodes” Synth. Met. 159 2326–2328 (2009).
73. J. H. Yim et al., “Fully Solution-Processed Semitransparent Organic Solar Cells with a Silver Nanowire Cathode and a Conducting Polymer Anode” Acs Nano **8** (3) 2857-2863 (2014).
74. J. Krantz et al., “Spray-Coated Silver Nanowires as Top Electrode Layer in Semitransparent P3HT:PCBM-Based Organic Solar Cell Devices” Adv. Funct. Mater. **23**, 1711–1717 (2013).
75. J-Y. Lee et al., “Semitransparent Organic Photovoltaic Cells with Laminated Top Electrode” Nano Lett. **10**, 1276–1279 (2010).
76. J-W. Kang et al., “All-spray-coated semitransparent inverted organic solar cells: From electron selective to anode layers band gap of the polymer is further decreased” Org. Electron. **13** 2940–2944 (2012).
77. F. Guo et al., “ITO-free and fully solution-processed semitransparent organic solar cells with high fill factors” Adv. Energy Mater. **3**, 1062–1067 (2013).
78. Z. M. Beiley et al. “Semi-transparent polymer solar cells with excellent sub-bandgap transmission for third generation photovoltaics” Adv. Mater. **25**, 7020-7026 (2013).
79. C.-C. Chen et al., “Visibly transparent polymer solar cells produced by solution processing” ACS Nano **6**, 7185–7190 (2012).
80. L. Dou, et al. “A selenium-substituted low-bandgap polymer with versatile photovoltaic applications” Adv. Mater. **25**, 825–831 (2013).
81. C.-C. Chueh, et al., “Toward high-performance semi-transparent polymer solar cells: optimization of ultra-thin light absorbing layer and transparent cathode architecture” Adv. Energy Mater. **3**, 417–423 (2013).
82. J. Meiss, et al., “Highly efficient semitransparent tandem organic solar cells with complementary absorber materials” Appl. Phys. Lett. **99**, 043301 (2011).
83. K.-S. Chen et al., “Semi-transparent polymer solar cells with 6% PCE, 25% average visible transmittance and a color rendering index close to 100 for power generating window applications” Energy Environ. Sci. **5**, 9551–9557 (2012).
84. C-C. Chen et al., “High-performance semi-transparent polymer solar cells possessing tandem structures” Energy Environ. Sci**. 6**, 2714-2720 (2013).

85. Z. Tang et al., “Semi-Transparent Tandem Organic Solar Cells with 90% Internal Quantum Efficiency” Adv. Energy Mater 2, 1467–1476 (2012).
86. W. Yu et al., “Simultaneous improvement in efficiency and transmittance of low bandgap semitransparent polymer solar cells with one-dimensional photonic crystals” Solar Energy Mater. Solar Cells **117**, 198–202 (2013).
87. W. Yu et al., “Semitransparent polymer solar cells with one-dimensional (WO3/LiF)N photonic crystals” Appl. Phys. Lett. **101** 153307 (2012).
88. Y. Long et al., “Optimizing one-dimensional photonic-crystals based semitransparent organic solar cells by tailoring reflection phase shift within photonic bandgap” Appl. Phys. Lett. **99**, 093310 (2011).
89. Y. Galagan et al., “Semitransparent organic solar cells with organic wavelength dependent reflectors” Appl. Phys. Lett. **98**, 043302 (2011).
90. D-D. Zhang et al., “Enhanced Performance of Semitransparent Inverted Organic Photovoltaic Devices via a High Reflector Structure” ACS Appl. Mater. Interfaces, **5**, 10185−10190 (2013).
91. L. Zuo et al. , “Microcavity-Enhanced Light-Trapping for Highly Efficient Organic Parallel Tandem Solar Cells” Adv. Mater. DOI: 10.1002/adma.201402782 (2014).
92. F. Pastorelli et al., “Enhanced Light Harvesting in Semitransparent Organic Solar Cells using an Optical Metal Cavity Configuration” Adv. Energy Mater. DOI: 10.1002/aenm.201400614 (2014).
93. C.-Y. Chang et al.,“A Versatile Fluoro-Containing Low-Bandgap Polymer for Efficient Semitransparent and Tandem Polymer Solar Cells” Adv. Funct. Mater. **23**, 5084-5090 (2013).
94. Y. Sun et al., “Inverted Polymer Solar Cells Integrated with a Low-Temperature-Annealed Sol-Gel-Derived ZnO Film as an Electron Transport Layer” Adv. Mater. **23**, 1679-1683 (2011).
95. R. R. Lunt. “Theoretical limits for visibly transparent photovoltaics” App. Phys. Lett. **101**, 043902 (2012).
96. F. Guo et al. “Fully solution-processing route toward highly transparent polymer solar cells” ACS Applied Materials and Interfaces, **6**, 18251-18257 (2014).

Pablo Romero-Gomez is a research fellow at the Institute Of Photonic Sciences-ICFO. He received his BS and MS degrees in physics from the University of Córdoba and Seville in 2006 and 2008, respectively, and his PhD degree in Science and Technology of New Materials from the Institute of Material Science of Seville-ICMS in 2011. His current research interests include photovoltaic solar cells, photonic management and fabrication of new nanomaterials.

Francesco Pastorelli is currently a postdoc researcher at the Danish Technical University in the energy conversion and storage department. In 2013 he received his PhD in a joint European program between Fresnel Institute, Marseille, and the Institute of Photonics Science, Barcelona. He was a visitor scientist at the Columbia University, New York, at the University of Tokyo and at the Italian Institute of Technology, Lecce. His research interests include light enhanced photovoltaic devices and printed devices.

Paola Mantilla-Perez is a PhD candidate at the Institute of Photonic Sciences. She received her BS degree in Electronic Engineering from the Universidad del Norte in Colombia, in 2007. Later in 2011, she received a MS degree in optics and photonics from the Karlsruhe University of Technology in Germany. Her current research include light management in organic tandem solar cells and all-solution-processed organic photovoltaics. She is an active student member of OSA, SPIE and EPS.

Marina Mariano is a postdoctoral researcher at the University of Yale in the Chemical Engineering department. She received her BS degree in physics from the University of Barcelona in 2008, and her MS degree in photonics from BarcelonaTech in 2009. In 2014 she has received her PhD degree in photonics from BarcelonaTech and ICFO-The Institute of Photonic Sciences. Her current research interests include optical enhancements for better light harvesting in solar cells.

Martinez-Otero is a postdotoral fellow at the Institute of Photonic Sciences (ICFO). He received his BS degree in Chemistry from the Universidad de Santiago de Compostela in 2000, and his PhD degree in Material Sciences from the Universitat

Autonoma de Barcelona in 2010 after several years working for the industry. He is the author or co-author of 15 journal papers and one book chapter. His current research interests include photovoltaics and printed electronics.

Xavier Elias is a Research Fellow at ICFO-The Institute of Photonic Sciences. He holds BS and MS degrees in Chemistry from the Autonomous University of Barcelona, and a PhD in chemistry from the same university, which he received in 2006. His current research is focused on novel energy materials, organic photovoltaics and water splitting using sunlight.

Rafael Betancur is an associate researcher at the Centro de investigación, innovación y desarrollo de materiales. He received his BS in engineering physics and MS in physics from the Universidad Nacional de Colombia in 2005 and 2008, respectively, and his PhD degree in photonics from the Institute of photonic sciences in 2013. His current research interests include development of low cost photovoltaic devices, photonic management and materials science.

Jordi Martorell received a PhD degree in Physics from Brown University (USA) in 1990. He became a UPC professor in 1999 and since 2005 he is group leader at ICFO. He has mainly focused his research into the experimental study of the optical control to shape the properties of photonic materials. Currently, the core of his research is focused to the study of photonics applied to enhance the performance of photovoltaics cells.

Caption List

Figure 1 PTB7:$PC_{71}BM$ cells incorporating **a**) a periodic 1-D photonic crystal of six layers, and **b)** a non-periodic multilayer of five layers. LRI and HRI indicate low and high refractive index, respectively. CBL indicates charge blocking layer. When the bottom CBL is an electron blocking layer the configuration is known to be a standard one, while when the top CBL is an electron blocking layer the configuration is known as inverted.

Figure 2 As a function of the number of layers numerically determined relative short circuit current (green solid dots) and luminosity (green circles) for

devices incorporating the non-periodic multilayer, and relative short circuit current (red solid squares) and luminosity (red empty squares) for devices incorporating optimal periodic 1-D photonic crystals of 2 and 3 periods. The short circuit currents are given relative to the corresponding one from an equivalent opaque cell.

Figure 3 Reflectivity of the periodic 1-D photonic crystal of four layers (red dashed line), of six layers (red solid line) and a non-periodic multilayer of five layers (green solid line). All three structures where designed to maximize the performance of the entire OPV device using the same inverse integration. The constraint of periodicity was removed for the last case.

Figure 4 a) Experimentally measured EQE for semi-transparent cells in the standard configuration when no photonic management is incorporated (red solid line), and when a 1-D non-periodic crystal of five layers is included (green solid line). Numerically predicted EQE for a semi-transparent standard cell incorporating a 1-D non-periodic crystal of five layers designed ad hoc to optimize visible transparency and PCE (green dashed line). **b**) Same as in a) but for an inverted configuration.

Figure 5 Schematic picture of a PTB7:$PC_{71}BM$ cell in a metal cavity configuration incorporating a periodic 1-D photonic crystal of six layers and an anti-reflection coating.

Figure 6 Experimentally measured EQEs of an opaque cell (black solid line), of a bare semi-transparent cell (red solid line) and a semi-transparent cell in a metal cavity configuration (green solid line), as the one shown in Figure 5, incorporating a periodic 1-D photonic crystal of six layers and an anti-reflection coating.

Table 1 Summary of high performance semitransparent OPV cells reported during the 2012-2014 period